



## ANALYSIS OF GEOTHERMAL WELL TEST DATA FROM THE ASAL RIFT AREA, REPUBLIC OF DJIBOUTI

**Daher Elmi**

Centre d'Etudes et de Recherches Scientifique de Djibouti – CERD  
P.O. Box 486, Djibouti  
République de Djibouti  
*daherelmihoussein@yahoo.fr*

### ABSTRACT

The Asal area has been described as a segment of the world oceanic rift system by earlier investigators. A total of six deep wells have been drilled in the area, the first two in 1975 and the last four in 1987 and 1988. Well Asal 2 was damaged, wells Asal 4 and Asal 5 were impermeable although very hot, but wells Asal 1, 3 and 6 have produced extremely saline fluids from 1000-1300 m depth where the aquifer temperature is about 260°C. Well test data from wells Asal 3, 4 and 6, including injection test data, draw-down test data, pressure build-up data and pressure interference data have been analyzed in order to estimate the reservoir properties of the Asal geothermal system. The permeability thickness of the deep geothermal reservoir is estimated to be about 4-8 Dm. A low storativity value of about  $2 \times 10^{-9}$  m/Pa reflects a reservoir thickness of about 250 m. During long-term exploitation a large pressure draw-down is observed in the reservoir. Wells Asal 3 and Asal 6 produce highly saline (120 g/l) reservoir fluid and the scaling of galena at high pressure reduces the discharge rate. Extensive exploration and field tests need to be performed to accurately estimate the actual size and capacity of the Asal reservoir. Laboratory studies should be conducted in order to find chemical inhibitors that may solve the scaling problem. If the outcome of these tests is positive, new production wells should be drilled. It is recommended that the suitability of a 130°C resource found between 400 and 600 m depth in the Asal area be studied for binary power production.

### 1. INTRODUCTION

The Republic of Djibouti (23,000 km<sup>2</sup>) is located in East Africa where three major extensional structures, the Red Sea, the East African rift and the Gulf of Aden, join forming the Afar Depression (Barberi et al., 1975). This particular area is characterized by the presence of geothermal resources revealed by numerous hot springs found in different parts of the country. The most active structure is the Asal Rift which is the westward prolongation of the Gulf of Aden - Gulf of Tadjoura Ridge.

Geothermal exploration in the Republic of Djibouti was initiated by drilling of two wells in the rift of Asal in 1975 (BRGM, 1980a) which located a deep reservoir at 1000 m depth with high salinity and temperature of 260°C. Additional geothermal exploration in the Republic of Djibouti consisted of drilling of two exploratory wells in the Hanlé plain, followed by four wells in the Asal Rift (Aquater,

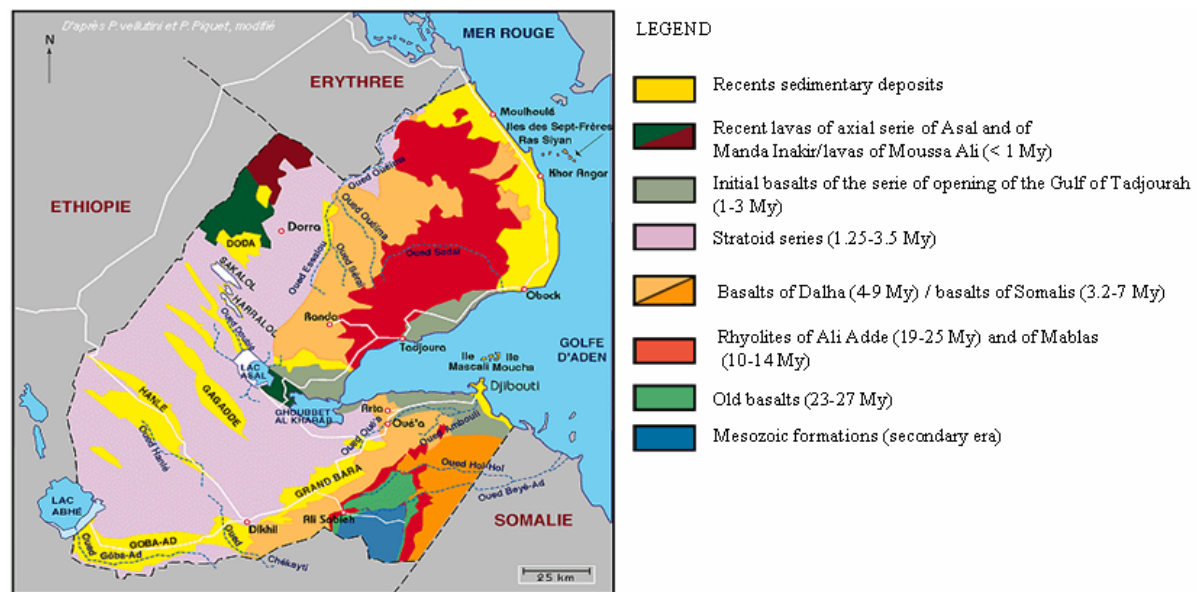


FIGURE 1: Geological map of the Republic of Djibouti

1989). The latter project started in December 1986 with the drilling of well Hanlé 1 on the Hanlé plain (Figure 1). On the basis of the low temperatures recorded in wells Hanlé 1 and 2 (72°C at 1400 m and 123°C at 2017 m, respectively), and considering that high-temperature fluids were known to exist in the Asal Rift (BRGM, 1980b), four wells were drilled in the Asal area.

The geothermal exploration programmes of the Asal area, including field studies and exploration drilling between 1970 and 1990, revealed the high salinity, deep Asal geothermal reservoir and other potential geothermal areas. However, all these investigations did not yet lead to any exploitation of the geothermal energy.

This report reviews available geological information on the Asal geothermal area and information on the geothermal wells in the area. The main purpose of the report was the analysis of well test data from wells in the area, including injection test data, draw-down test data, pressure build-up data and pressure interference data in order to estimate the reservoir properties of the Asal geothermal system. Some well output data are also interpreted and simulated by a well-bore simulator. Finally, some recommendations concerning future development of the Asal geothermal resources are presented.

## 2. THE ASAL GEOTHERMAL FIELD

### 2.1 Geograpy

The Asal geothermal system is located on the isthmus between Lake Asal and Ghoubet al Kharab gulf (Figure 2) at a distance of about 120 km from Djibouti City. Altitudes range from -151 m at Lake Asal to +300 m at the highest point of the Rift valley floor. The area is bounded by the high plateaus of Dalha to the north (above 1000 m elevation) and by 400-700 m high plateaus to the south, which separate Asal from the Gaggade and Hanle sedimentary plains (Figure 1).

The region is arid desert, with an average rainfall of 79 mm per year. Hydrogeological studies of the region show a general groundwater flow toward Lake Asal, which is the lowest point of the area, and is occupied by a salt lake saturated in sodium chloride and calcium sulphates. The area is controlled by tectonic faults, still active.

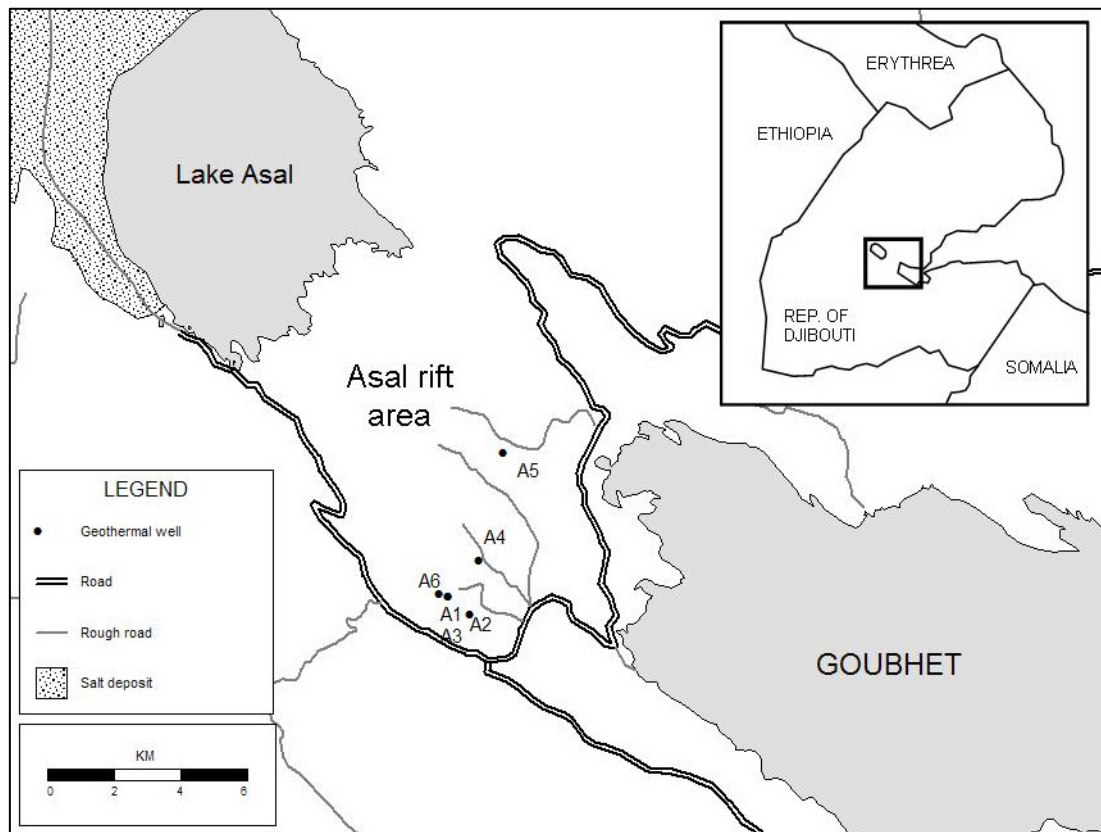


FIGURE 2: Location of geothermal boreholes in the Asal Rift area

## 2.2 Geology

The Asal Rift is tectonically the most active structure in the zone of crustal divergence in Afar (Figure 3). The Asal area constitutes a typical oceanic type rift valley, with a highly developed graben structure displaying axial volcanism. The Asal series are relatively complex in structure, because of different series of active volcanism in recent Quaternary times, each with very different characteristics depending on the sites of appearance. Generally, the Asal series are composed of porphyritic basalt formations and hyaloclastites.

The initial basalt series are an ensemble of piles of fine flows with phenocrystal of plagioclases and olivine. The stratoid series are essentially constituted by basalts, where the top series

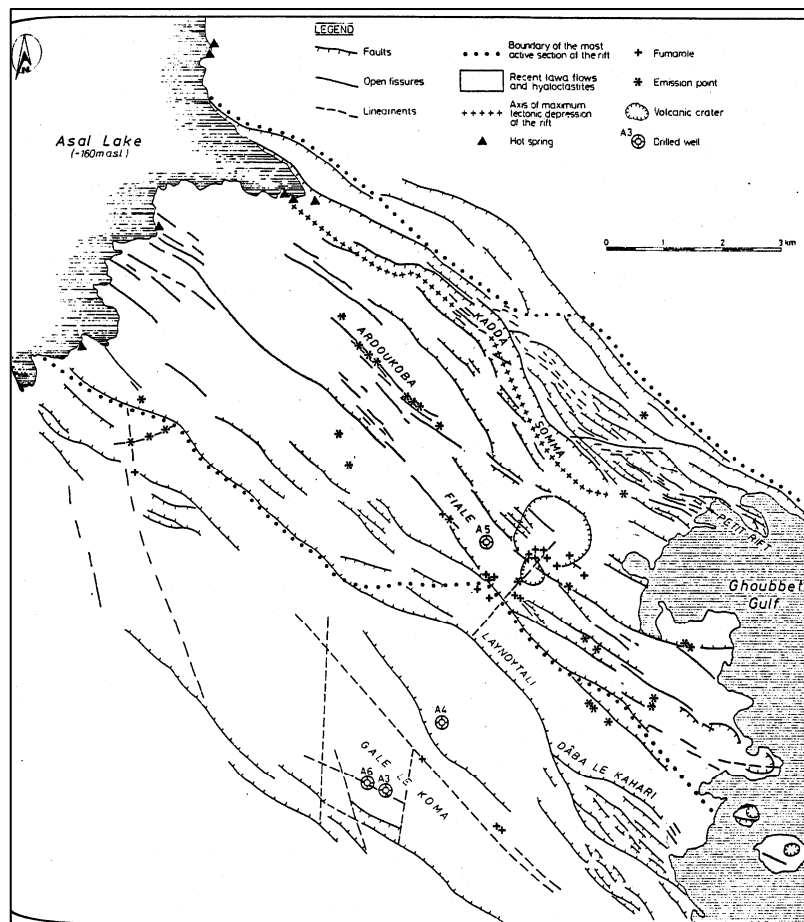


FIGURE 3: Structural map of the Asal area

is marked by Pleistocene clays. The basalt series of Dalha are characterized by sedimentary layers in-between the basalt flows.

Three main geological formations are known in the region and intersected by the wells. These are the Asal series (recent basalts on the geological map in Figure 1) with volcanism dating from the last 800,000 years (volcanism of the external margins of Asal, central volcanism and axial volcanism); the initial basalts series, or the stratoid basalts series, covering the period from 3.4 to 1 My; and the Dalha basalts series, dating between 9 and 3.4 My.

### 2.3 Geochemistry

The main results of geochemical studies of water from the Asal area are (Correia et al., 1985; Aquater, 1989):

- According to a study performed on samples collected from shallow aquifers from wells Asal 1, 2, 3, 4 and 6, and deep water samples from well Asal 3, as well as from samples of Lake Asal, it appears that all aquifers encountered are mainly recharged by sea water (Aquater 1989).
- Asal geothermal fluid originates through mixing of sea water and high TDS continental water of meteoritic origin.
- The geothermal fluid is not produced by the evaporation of sea water as in the case of the Asal Lake Na-Cl brine.
- The equilibrium temperature calculated from all reactive gaseous species ( $H_2O$ ,  $CO_2$ ,  $H_2$ ,  $CH_4$ ,  $CO$ ,  $N_2$ ,  $NH_3$ ), apart from  $H_2S$ , is about  $260^\circ C$  which is compatible with the temperature measured in the reservoir.
- The waters in Lake Asal are composed of very concentrated sea water due to evaporation and its  $CaSO_4$  content is modified owing mainly to precipitation. Deep geothermal waters seem to have no contact with Lake Asal waters and the Ca/Mg ratio is extremely different.
- Contrary to what was expected the fluids collected in well Asal 5 showed that the water at the centre of the rift has a much higher salinity than water at the borders.

### 2.4 Geophysical investigations

The results of a gravimetric survey (BRGM, 1980a) exhibits three main characteristics (Jalludin, 2002). The anomalies' principal direction appear in good accordance with the principal tectonic trend of the rift, NW-SE, and high horizontal gradients are aligned with the main axis of recent fractures, thus confirming the existence of these geological structures at depth. Secondly, numerous anomalies demonstrated by the survey reflect the local heterogeneity and their superficial origin in conformity with the geological observations, showing numerous structural units and a particularly dense fracture network. Finally, in the central part of the rift a clear anomaly corresponds to the principal inflow of magma where recent volcanic activities were observed.

The transversal magneto-telluric profile in the Asal rift generally showed conducting layers underlying resistant layers in some areas in relation to the presence of hyaloclastites overlain partially by recent basaltic formations. The study mainly points out the heterogeneity of the structures. The correlation between the different measuring stations is relatively difficult due to variations in thicknesses. Another profile in the vicinity of the recent Ardoukoba volcano suggests the presence of saline water in hyaloclastites, basalts, scorias and fissures.

Spontaneous polarisation (SP) profiles measured across the rift clearly describe a SP anomaly near the recent volcano of Ardoukoba. The interpretation of the profiles indicates that the general anomaly in the central part of the rift results from a thermal source. This signifies that the heat flow is generally high in this region.

### 3. WELL INFORMATION

Some basic information on the six wells drilled in the Asal geothermal area is presented in Table 1.

#### 3.1 Wells locations

The three boreholes Asal 1, 3 and 6 are located in the southern zone of the Asal rift, inside the half circle of hyaloclastite known as Gale le Koma. Wells Asal 1 and 3 are only 30 m apart; so in the following discussions only data of well Asal 3 will be considered. The distance between Asal 3 and 6 is approximately 300 m, along a line striking NW-SE. The two sites, Asal, 1/3 and 6 are located near a NW-SE fracture. Well Asal 2 is located 800 m southeast of the Asal 3 site. Asal 4 is located about 2 km north-northeast of the site of Asal 3 and 6, close to a NW-SE fracture. It is located on the same tectonic segment as the site of Asal 3 and 6. A major tectonic step-out is located 3 km further to the northeast; and well Asal 5 is located further away in the same direction at the axis of the rift. One can also note that well Asal 5 is located nearly 500 m from a major active fault.

#### 3.2 Main aquifers

Geological series distinguished from drilling samples are essentially based on the lithological characteristics and on the mineralogy. According to observations at the surface, the stratoide series and the more ancient Dalha basalts are separated by a layer of compact and grey clay. This clay layer was identified in the cuttings and corresponds to a quiet period with regard to tectonics and volcanism.

The stratigraphy encountered in the wells confirms what was expected from surface studies except in well Asal 5 where it was difficult to distinguish between the Asal series and Dalha series. All the feed zones encountered during drilling of the 6 wells are summarised in Table 1.

TABLE 1: Stratigraphy of Asal wells

Wells	Coordinates			Depth (m)	Feed zones (m)	Aquifer formations
	x (m)	y (m)	z (m a.s.l.)			
Asal 1	224781.47	1277342.33	191.026	1146	See Asal 3	
Asal 2	225429.28	1276814.12	187.63	1554	250-500	Stratoid basalt series
Asal 3	224800.36	1277342.35	192.665	1316	240-250 400-460 540-550 1050-1075 1225-1250 1275-1316	Contact hyaloclastite/scoria A.S. Rhyolite of stratoid series Trachyte of stratoid series  Dalha basalts series
Asal 4	225740.92	1278432.56	201.607	2013	250-420	Basalts, and contact basalt-hyaloclastite of Asal Series
Asal 5	226303	1281353	125	2105	200-500	Basalts, trachytes and alluvium of Asal Series
Asal 6	224525.25	1277427.46	183.223	1761	220-270 400-600 1000-1300	Scoria of stratoid series Rhyolite/trachyte stratoid series Dalha basalts series

## 4. WELL TESTING

### 4.1 Well test theory

In a well test the pressure response of a reservoir during production or injection is monitored. Well testing is conducted in order to estimate reservoir properties and the conditions and flow capacity of a well. The most important properties are the permeability-thickness and the formation storativity. These are not evaluated directly from the data. The data has to be interpreted with the most appropriate model, resulting in average values. So the properties are model dependent. Definitions of variables used in the following sections are also given in Nomenclature.

#### 4.1.1 Pressure diffusion equation

The basic equation of well testing theory is the pressure diffusion equation. It can be used to calculate pressure ( $P$ ) in a reservoir at a certain distance ( $r$ ) from a production well producing at the rate ( $q$ ) after a given time ( $t$ ). The most used solution of the pressure diffusion equation is the so called Theis solution or the line source solution.

The three governing laws that are used in deriving the pressure diffusion equation are the following (Horne, 1995):

Law conservation of mass inside a given control volume, or;

$$\text{Mass flow in} - \text{Mass flow out} = \text{Rate of change of mass within the control volume}$$

Law of conservation of momentum - Darcy's law, or;

$$q = 2 \pi r h \frac{k}{\mu} \frac{\partial P}{\partial r}$$

where  $q$  = Volumetric flowrate ( $\text{m}^3/\text{s}$ );  
 $h$  = Reservoir thickness (m);  
 $k$  = Formation permeability ( $\text{m}^2$ );  
 $P$  = Reservoir pressure (Pa);  
 $r$  = Radial distance (m);  
 $\mu$  = Dynamic viscosity of fluid (Pas).

Equation of state of the fluid:

$$c = \frac{1}{\rho} \left( \frac{\partial \rho}{\partial P} \right)_T$$

where  $c$  = Compressibility of fluid ( $\text{Pa}^{-1}$ );  
 $\rho$  = Density of fluid ( $\text{kg}/\text{m}^3$ );  
 $T$  = Temperature ( $^{\circ}\text{C}$ ).

Initially the following simplifying assumptions are used:

- The flow is considered isothermal,
- The reservoir is considered homogeneous and isotropic,
- The producing well penetrates the entire formation thickness,
- The formation is completely saturated with a single fluid.

Combining the above equations and using the above assumptions, the pressure diffusion equation results:

$$\frac{\partial}{\partial r} \left( r \frac{\partial P(r,t)}{\partial r} \right) = \frac{\mu C_t}{k} \frac{\partial P(r,t)}{\partial t}$$

where  $C_t$  = Total compressibility ( $\text{Pa}^{-1}$ ).

Theis (1935) proposed an integral solution for this equation for:

- Initial condition:

$$P(r, t) = P_i \quad \text{for} \quad t = 0 \quad r > 0$$

- Boundary conditions :

$$\text{i) } P(r, t) = P_i \quad \text{for} \quad r \rightarrow \infty \quad t > 0$$

$$\text{ii) } q = 2\pi r h \frac{k}{\mu} \frac{\partial P}{\partial r} \quad \text{for} \quad r \rightarrow 0 \quad t > 0$$

The solution to the radial diffusion equation with these boundary and initial conditions is given by:

$$P(r, t) = P_i + \frac{q\mu}{4\pi k h} Ei \left( \frac{-\mu C_t r^2}{4kt} \right)$$

where  $Ei(-x) = -\int_x^\infty \frac{e^{-u}}{u} du$  is the exponential integral function.

If  $t > 100 \frac{\mu C_t r^2}{4k}$  the exponential integral function can be expanded by a convergent series and thus, the Theis solution, for a pumping well with skin gives the total pressure change as:

$$\Delta P_t = -\frac{2.303q\mu}{4\pi h k} \left[ \log \left( \frac{\mu C_t r_w^2}{4kt} \right) + \frac{0.5772 - 2s}{2.303} \right]$$

where  $s$  = Skin factor which describes pressure changes next to a well because of reduced/increased permeability in that region (skin).

#### 4.1.2 Semi-logarithmic well test analysis

A plot of the Theis solution for  $\Delta P$  vs.  $\log t$  gives a semi-log straight line with a slope  $m$  per log cycle for the infinite acting radial flow period of a well ( $t > 100 \mu C_t r^2 / 4k$ ). This approach is referred to as a semi-log analysis.

$$m = \frac{2.303q\mu}{4\pi k h} \text{ (Pa/log cycle)}$$

The skin factor is determined by:

$$s = 1.151 \left[ \frac{\Delta P}{m} - \log \left( \frac{k}{\phi \mu C_t r_w^2} \right) - \log(t) - 0.351 \right]$$

Semi-log analysis is based on the interpretation of the semi-log straight line response that represents the infinite acting radial flow behaviour of the well. However, as the wellbore has finite volume, it

becomes necessary to determine the duration of the wellbore storage effect or the time at which the semi-log straight line begins.

The wellbore storage effect is identified as a unit slope line on a  $\log(\Delta P)$  vs.  $\log(t)$  graph. After  $1\frac{1}{2}$  log cycles from the end of the unit slope line, the semi-log straight line is expected to start.

#### 4.1.3 Type curve methods

Well test analysis often makes use of dimensionless variables. The importance of dimensionless variables is that they simplify the reservoir models by combining the reservoir parameters (such as  $k$ ,  $c_i$ , etc.) thereby reducing the total number of unknowns. They have the additional advantage of providing model solutions that are independent of any particular unit system. It is an inherent assumption in the definition that permeability, viscosity, compressibility, porosity, and thickness are all constants. Thus we define:

$$P_D = \frac{2\pi kh}{q\mu} \Delta P = \text{dimensionless pressure change};$$

$$t_D = \frac{kt}{C_i \mu r_w^2} = \text{dimensionless time};$$

$$r_D = r/r_w = \text{dimensionless radial distance from the active well.}$$

Generally, the procedure for type curve analysis can be outlined as follows:

- The data is plotted as  $\log \Delta P$  vs.  $\log \Delta t$  on the same scale as that of the type curve.
- The curves are then moved, one over the other, by keeping the vertical and horizontal grid lines parallel until the best match is found.
- The best match is chosen and the pressure and time values are read from fixed points on graphs,  $\Delta P_M$ ,  $P_{DM}$ ,  $\Delta t_M$ , and  $t_{DM}$ .
- For an infinite acting system, the transmissivity,  $T$ , is evaluated from:

$$T = \frac{kh}{\mu} = \frac{q}{2\pi} \left( \frac{P_D}{\Delta P} \right)_M$$

and the storativity,  $S$ , is calculated as:

$$S = C_i h = \frac{kh}{\mu r_w^2} \left( \frac{\Delta t}{t_D} \right)_M$$

#### 4.1.4 Multirate drawdown test - Odeh and Jones's method

When a well-test is conducted in steps with different flowrates, Odeh and Jones's method may be used (Horne, 1995). The following equation, based on the principle of superposition, is used:

$$\frac{P_i - P_{wf}(t)}{q_N} = \frac{2.303\mu}{4\pi kh} \sum_{j=1}^N \left[ \frac{(q_j - q_{j-1})}{q_N} \log(t - t_{j-1}) \right] + b'$$

- where
- $P_i$  = Initial pressure (Pa);
  - $P_{wf}(t)$  = Flowing pressure well at time  $t$  (Pa);
  - $N$  = Number of flowrates;
  - $q_j$  = Flow step between  $t_{j-1}$  and  $t_j$  ( $\text{m}^3/\text{s}$ );
  - $t_j$  = Time at the flowrate  $q_j$  (s).

A plot of  $\frac{P_i - P_{wf}(t)}{q_N}$  vs.  $\sum_{j=1}^N \left[ \frac{(q_j - q_{j-1})}{q_N} \log(t - t_{j-1}) \right]$  should show a straight line with slope  $m'$ :

$$m' = \frac{2.303\mu}{4\pi kh} \quad (\text{Pa}/(\text{m}^3/\text{s}))$$

#### 4.1.5 Buildup test - Horner method

This is a particular case of superposition in time for production and shut-in. The effect of these two flowrates can be represented by a well which produces for a time  $t_p$ , at a rate  $q$ , and then is shut-in for time  $\Delta t$ .

$$\Delta P_{ws} = \frac{2.303q\mu}{4\pi kh} \log\left(\frac{t_p + \Delta t}{\Delta t}\right)$$

where  $\Delta P_{ws}$  = Pressure change after time  $t_p$  (Pa).

A plot of  $\Delta P_{ws}$  vs.  $\log\left(\frac{t_p + \Delta t}{\Delta t}\right)$  should show a straight line with a slope  $m$  when the reservoir behaves as infinitely acting:

$$m = \frac{2.303q\mu}{4\pi kh}$$

If a series of  $N$  different flowrates have been measured prior to shut-in, the well shut-in pressure assuming infinite acting (semi-log) behaviour can be written as:

$$\Delta P_{ws} = m' \sum_{j=1}^N \frac{q_j}{q_N} \log\left(\frac{t_N - t_{i-1} + \Delta t}{t_N - t_j + \Delta t}\right)$$

where  $q_N$  = The last rate the well flowed at before being shut.

Thus, a plot of  $\Delta P_{ws}$  vs.  $\sum_{j=1}^N \frac{q_j}{q_N} \log\left(\frac{t_N - t_{i-1} + \Delta t}{t_N - t_j + \Delta t}\right)$  should show the slope  $m'$ :

$$m' = \frac{2.303q\mu}{4\pi kh}$$

#### 4.1.6 Fractures

Fractures can be detected in well testing as follows (Horne, 1995):

- Bi-linear flow: this response is detected by a straight line pressure response with slope  $\frac{1}{4}$  at an early time on  $\log(\Delta P)$  vs.  $\log(\Delta t)$  graph.
- Linear flow: this response is detected by a straight line pressure response with slope  $\frac{1}{2}$  at an early time on  $\log(\Delta P)$  vs.  $\log(\Delta t)$  graph.
- Radial flow: at late times the pressure response may develop into a radial flow response (This solution).

## 4.2 Analysis of Asal 3 well tests

Well Asal 3 was drilled in 1987 to a total depth of 1316 m. The well is cased with 9-5/8" casing to 1016 m and it is open hole between 1016 and 1316 m. For all the transient pressure tests the measurements of pressure were made at 1075 m depth, thus near the upper permeable zones of the deep reservoir in the well (Table 1). The data correspond essentially to the investigation phase carried out by ISERST/AQUATER between 1987 and 1988 (Aquater, 1989).

The curves of four drawdown tests are presented on a semi-logarithmic graph in Figure 4. Notice that the effect of the capacity of the borehole is unimportant and seems to be over after a very short period, less than ten minutes. No fracture effects are seen. Short wellbore storage period indicates a good hydrodynamics characteristic of the reservoir near the wellbore.

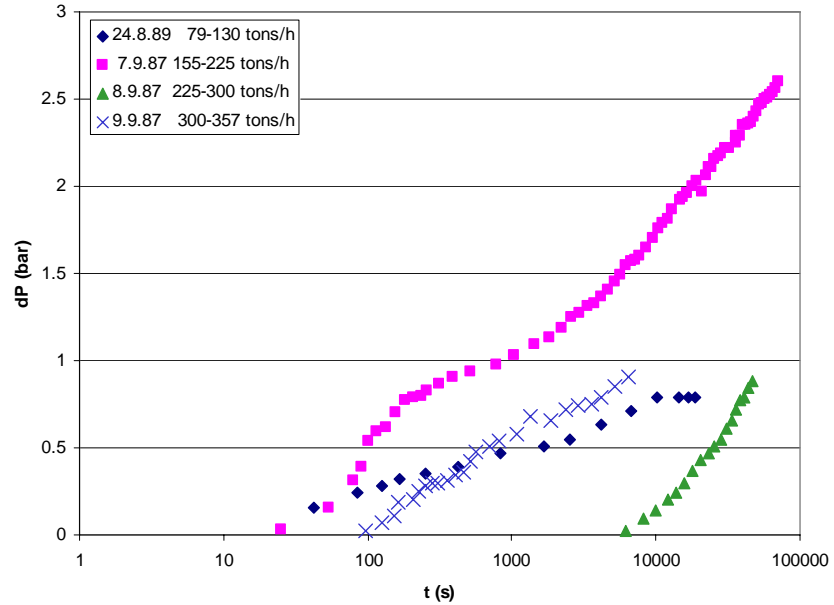


FIGURE 4: Semi-log graph of drawdown tests for Asal 3 at different times

Considering the high salinity (120 g/l) and the temperature (263°C) of the fluid in the reservoir, the following values for the dynamic viscosity and the density of fluid were used for the interpretations:

$$\mu = 1.4 \times 10^{-4} \text{ Pa s} \quad \rho = 890 \text{ kg/m}^3$$

For the type curve match, the model for a single well in an infinite system with wellbore storage and skin included (Argawal et al., 1970) was used with:

$$C_D = \frac{C}{2\pi\phi h C_t r_w^2}$$

- where  $C_D$  = Dimensionless wellbore storage coefficient;  
 $C$  = Wellbore storage coefficient ( $\text{m}^3/\text{Pa}$ ) =  $\pi r_w^2 / (9.81\rho)$  for free liquid level;  
 $r_w$  = Radius of well = 0.12 m;  
 $\phi$  = Porosity = 0.05;  
 $h$  = Thickness = 250 m;  
 $C_t$  = Total compressibility =  $\phi C_w + (1 - \phi)C_r$ .

Typical values of  $C_w$  (compressibility of water at 263°C) =  $1 \times 10^{-9} \text{ Pa}^{-1}$  and the compressibility of basalt rock  $C_r = 2 \times 10^{-11} \text{ Pa}^{-1}$  are used. The results of interpretation of the drawdown tests with the semi-log method, the type curve match and for multiflowrates (shown in Figure 5) are presented in Table 2.

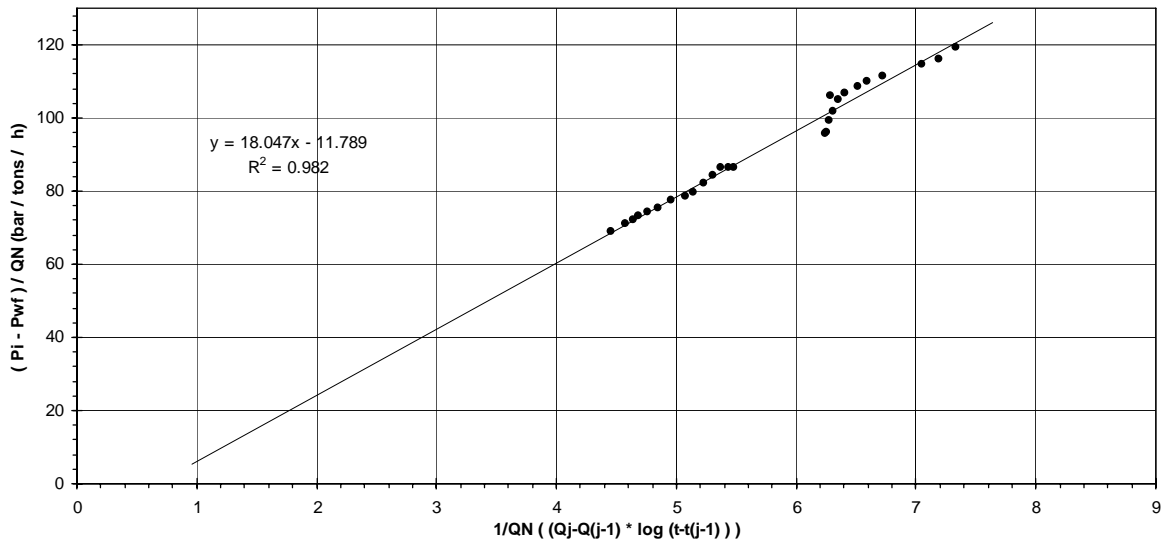


FIGURE 5: Analysis of multirate drawdown test in well Asal 3

TABLE 2: Results from analysis of drawdown tests data for Asal 3

Date	q (tons/h)	Δq (tons/h)	Semi-log		Type curve method		
			m (Pa)	kh (Dm)	$\left( \begin{matrix} t_D; P_D \\ t(s); \Delta P(Pa) \end{matrix} \right)$	Skin	kh (Dm)
24.8.87	Multiple	51	$0.29 \times 10^5$	14	$\left( \begin{matrix} 1 \times 10^6; 10 \\ 2000; 2.6 \times 10^5 \end{matrix} \right)$	-5	13.6
24.8.87		18.05 (bar/(tons/s))	16				
7.9.87	155-225	70	$0.976 \times 10^5$	5.75	$\left( \begin{matrix} 1 \times 10^7; 10 \\ 72000; 7 \times 10^5 \end{matrix} \right)$	-5	7
8.9.87	225-300	75	$1.43 \times 10^5$	4.2	$\left( \begin{matrix} 10; 10 \\ 5000; 12 \times 10^5 \end{matrix} \right)$	-5	4.3
9.9.87	300-357	57	$0.33 \times 10^5$	14	$\left( \begin{matrix} 1 \times 10^6; 1 \\ 600; 0.25 \times 10^5 \end{matrix} \right)$	-5	15.9

From these results, we distinguish two ranges for the transmissivity values, i.e. 14-16 Dm at 50-57 tons/h and 4-6 Dm for 70-75 tons/h. This demonstrates the following:

- The heterogeneity of the reservoir,
- It is possible that this results from a zone of higher permeability in the vicinity of the well, which controls the lower flowrate tests, while the zone of influence becomes larger (and permeability lower) as flowrate increases.

The estimated skin factor is negative (-5). Skin is an additional pressure change relative to the normal pressure change in the near vicinity of the well due to production. The negative factor obtained indicates that the well is in good communication with the reservoir.

The results of the build-up tests in well Asal 3 are presented in Table 3.

TABLE 3: Results of analysis build-up test data for Asal 3

Date	$q$ (ton/h)	$\Delta q$ (ton/h)	$m$ (Pa)	$kh$ (Dm)
9.9.87	357-0	357	$3.55 \times 10^5$	8
26.12.87	87-0	87	$1.42 \times 10^5$	5

The two build-up tests (Figure 6) have been interpreted by the Horner method. The values of transmissivity (5 and 8 Dm) are in a better agreement with the lower permeability values estimated for well Asal 3 on basis of the drawdown tests (Table 2). The measurements made during the build-up period are controlled by the global behaviour of the aquifer. That is why the calculated  $kh$  is less indicating that the zone with  $kh$  of the order of 14-16 Dm has limited extent. The tests were made at the same level, (1075 m) as the production tests, indicating that there is a large drawdown in the reservoir, around 10 bar-g.

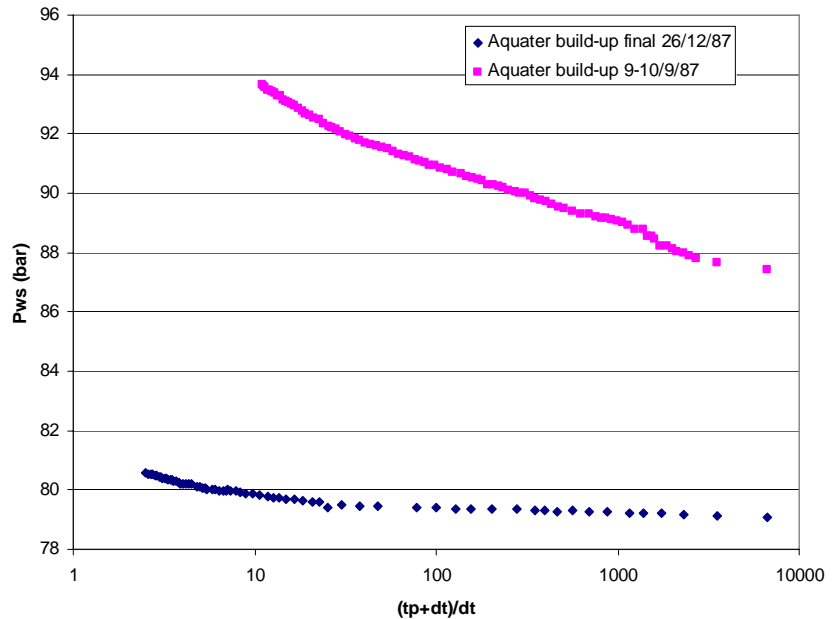


FIGURE 6: Well Asal 3 build-up tests

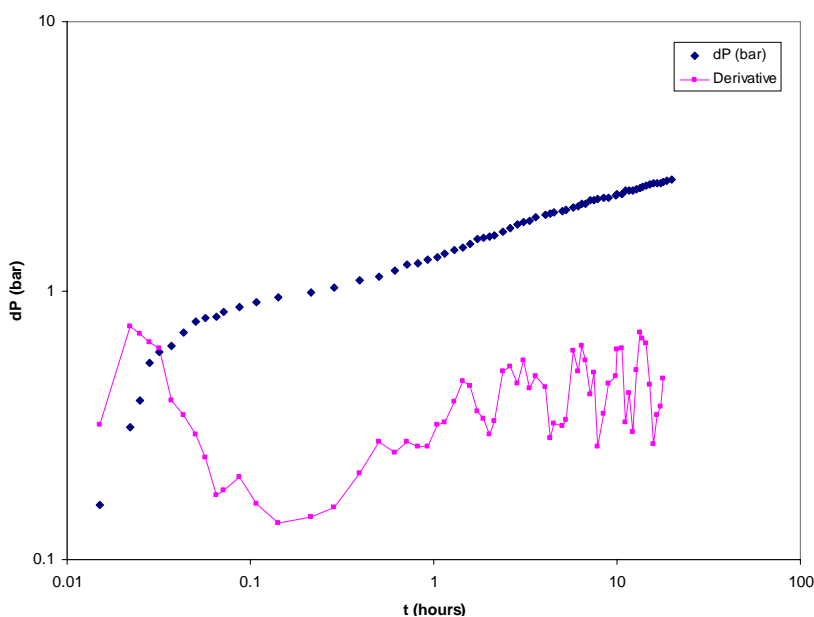


FIGURE 7: Composite plot of pressure change and the pressure derivative functions vs. time for the Asal 3 production build-up test of September 7 1987

None of the test data for Asal 3 show a pressure variation with a slope equal to 1 on a log-log graph. This shows that the effect of wellbore storage lasts only for a few minutes. It is not clear whether the producing zones found in this borehole correspond to fractures. Although it is not definitively excluded considering the low skin factor and the geologic characteristics in the area, it seems that dual porosity behaviour is dominant. This is indicated by Figure 7 which shows a minimum on a derivative plot.

### 4.3 Analysis of Asal 4 well tests

Well Asal 4 was drilled in 1988 to a total depth of 2013 m. The well is cased with 9<sup>5</sup>/<sub>8</sub>" casing to 2013 m. An injection test was performed in well Asal 4 with an injection rate of 70 m<sup>3</sup>/hour for 113 minutes (Figure 8). The variations of pressure were measured during and after the injection for 220 minutes. The fluid used for the injection was sea water thus having characteristics very different from those of the fluid in the reservoir. Nevertheless, the data allows to carry a valid interpretation by classic well test analysis methods.

Figure 8 shows that the effect of wellbore storage is very important. After 1½ log cycle from the end of the unit slope line, the semi-log straight line is expected to start. Data for the infinitely acting radial flow period are relatively limited in this case and the distribution of the experimental data is not very regular. This can be explained by the difficulties in maintaining a constant flowrate. For this reason it is difficult to use the match curve method for Asal-4. The log-log graph shows a straight line pressure with a slope ½, thus indicating the presence of fractures.

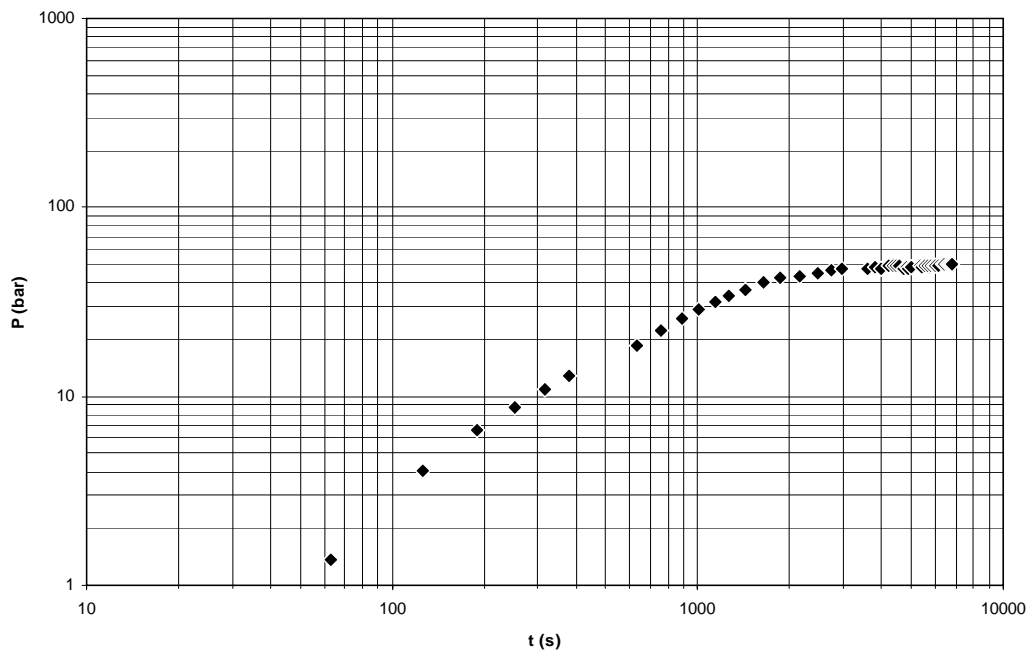


FIGURE 8: Log-log graph for the Asal 4 injection test at 70 m<sup>3</sup>/h

The results of the injection test and the recovery test using the Horner method (Table 4) show a low transmissivity (0.4-0.7 Dm). This value is very low with regard to that of Asal 3 and is in agreement with the injectivity indices calculated for Asal 4 and Asal 3, 1.4 m<sup>3</sup>/ h.bar and 100 m<sup>3</sup>/h bar, respectively. Production from well Asal 4 could not be initiated, most likely due to the low transmissivity. From the injection and recovery parts, the estimated skin factor is -4.6. Hence the well appears to be in a good connection with the reservoir.

TABLE 4: Results of analysis of injection and recovery test data for Asal 4

Date	q (m <sup>3</sup> /h)	Injection test		Recovery test		Horner plot	
		m (bar)	kh (Dm)	m (bar)	kh (Dm)	m (bar)	kh (Dm)
18.2.87	70	5.22	0.41	3.4	0.61	6.57	0.76

**4.4 Analysis of well Asal 6**

Well Asal 6 was drilled in 1989 to a total depth of 1716 m. The well is cased with a 9<sup>5</sup>/<sub>8</sub>" casing to 388 m depth and with a 7" liner between 364 and 919 m. It is an open hole from 919 m to 1761 m. Asal 6 was drilled about 300 m west-northwest of well Asal 3. It encountered permeable zone below 1315 m which is the depth of Asal 3. Thus Asal 6 can be expected to have a higher productivity than Asal 3. Several multirate tests (Figure 9), drawdown and interference tests (Figure 10) were carried out in order to determine the characteristics of the borehole (Table 5).

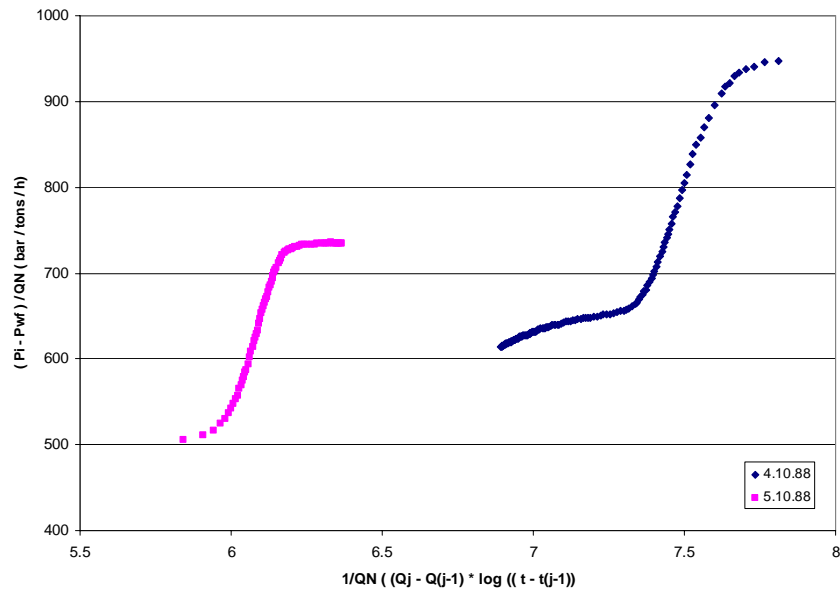


FIGURE 9: Data from multirate drawdown tests in Asal 6 at two different dates

TABLE 5: Results of analysis of different pressure transient tests in well Asal 6

Date	q (tons/h)	Δq (tons/h)	Semi-log	
			m (Pa)	kh (Dm)
4.10.88	Multiple		39.4 (bar/tons/s)	6.2
5.10.88	Multiple		39.5 (bar/tons/s)	6.3
5.10.88	65.2-78.3		0.13×10 <sup>5</sup>	8
5.10.88	115.2-0	13.1	1.22×10 <sup>5</sup>	7.5
1990	(Asal 3 shut-in)	115.2	(14 m)	

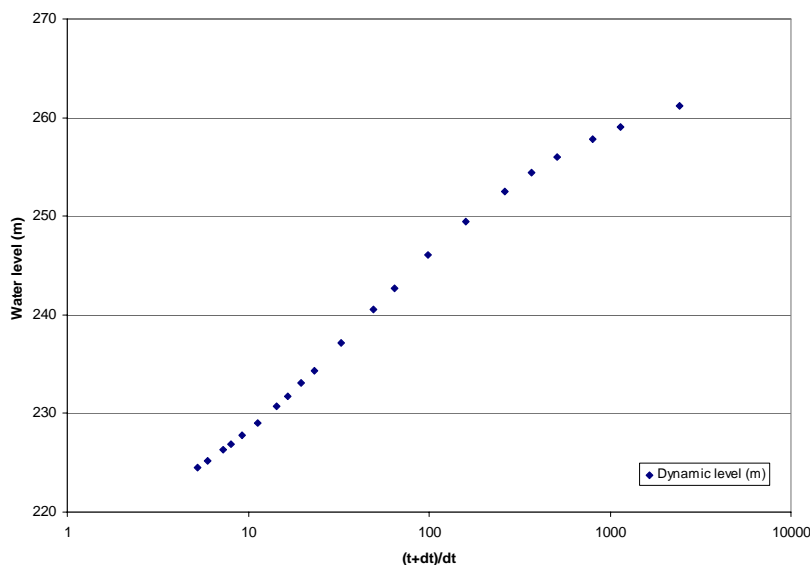


FIGURE 10: Interference test between Asal 6 and Asal 3 (Asal 3 shut-in)

From the water level recovery in well Asal 6 when well Asal 3 was shut-in (Figure 10), a formation storage coefficient value of  $6 \times 10^{-9}$  m/Pa was obtained; there is no skin factor for interference tests. From the drawdown test of 5.10.88 we have an estimation of a skin factor of around 30. It is necessary to note that several matching curves are possible and that this value is uncertain. A very high skin factor indicates a decrease of the formation permeability due to partial sealing of the invaded zone. From the

interference test, a storage coefficient of  $OC_h = 1.93 \times 10^{-9}$  m/Pa is estimated. Based on a total compressibility of about  $6.9 \times 10^{-11}$  Pa<sup>-1</sup>, the value obtained for porosity-thickness  $Oh$  is estimated to be 28 m. For a typical value for basalt porosity of 10%, the thickness of the reservoir is, therefore, estimated around 250 m.

The transmissivity estimates are of the same order as the global transmissivity calculated for Asal 3. For these various tests the transmissivity for well Asal 6 varies in the range from 6.2 to 8 Dm. In the region around wells 1, 3 and 6, the global transmissivity in the production interval down to 1600 m depth is thus estimated to be on the order of 4- 8 Dm.

## 5. FLOW TESTING OF WELL ASAL 3

### 5.1 Discharge measurement techniques

To start well Asal 3 flowing, the well was pressurized for one week to between 40 and 60 bars with an injection of air. The gas was slowly bled off but no discharge resulted. Then the airlift method was tried successfully.

During the production test, it was determined from the measured dynamic temperature and pressure conditions in the well during discharge (Figures 11 and 12, respectively) that well Asal 3 had liquid flow in the lower section of the well and two-phase boiling flow in the upper section. The boiling level was between 650 and 750 m during the measurements with the boiling level becoming deeper as drawdown increased.

After separation of the steam-water mixture into a flow of water and a flow of steam from a separator at atmospheric pressure (silencer), the water phase was measured using the weirbox method and steam flow by critical lip pressure before being discharged into the air.

The lip pressure method is based on an empirical formula developed by Russel James (see Grant et al., 1982). The lip pressure method is not quite as accurate as the separator method but is commonly used because a minimum of hardware and instrumentation is required to obtain good results.

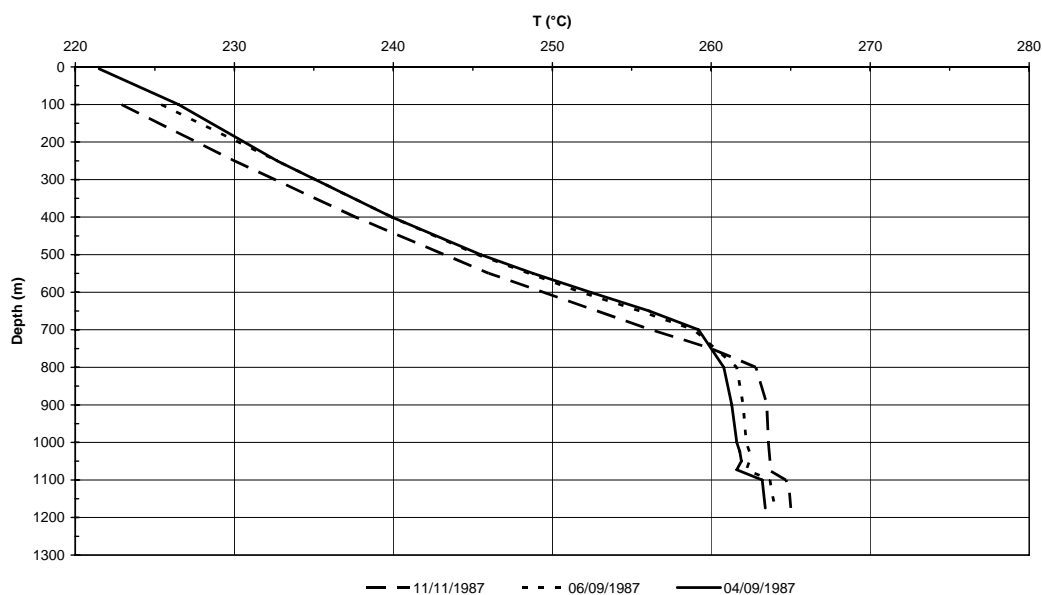


FIGURE 11: Temperature profiles during discharge testing

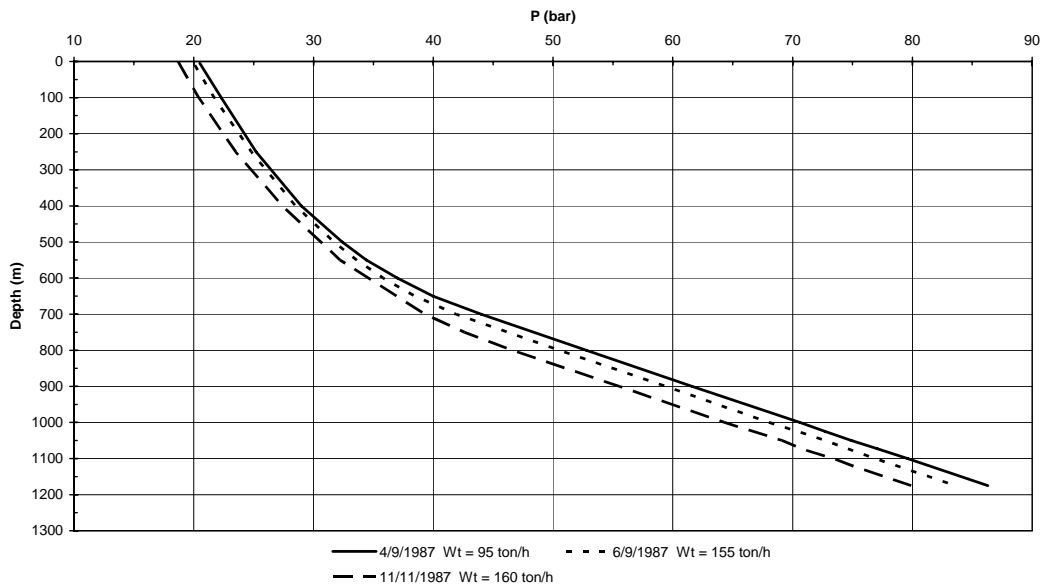


FIGURE 12: Pressure profiles during discharge testing

Assuming that we have a fairly large amount of steam/water mixture flowing at sonic velocity through an open-ended pipe to the atmosphere, the absolute pressure at the external end of the pipe is then proportional to the mass flowrate and enthalpy. The formula that Russel James deduced is:

$$\frac{W_t H_t^{1.102}}{A P_{lip}^{0.96}} = 1680$$

where  $P_{lip}$  = Lip pressure at the end of the pipe (MPa);  
 $W_t$  = Total mass flowrate (kg/s);  
 $A$  = Cross-sectional area of the lip (cm<sup>2</sup>);  
 $H_t$  = Total fluid enthalpy (kJ/kg).

When the water flow  $W_w$  (kg/s), from the atmospheric silencer and the lip pressure are known, the total fluid enthalpy is estimated by:

$$\frac{W_w}{A P_{lip}^{0.96}} = Y = \frac{0.74 (2675 - H_t)}{H_t^{1.102}}$$

The value for  $H_t$  is usually determined by iteration from the above equation. This equation can be solved for  $H_t$  between 400 and 2800 kJ/kg as a function of  $Y$  with an accuracy of 1.5% (Grant et al., 1982) by:

$$H_t = \frac{2675 + 365 Y}{1 + 3.1 Y}$$

The water flow  $W_w$  is related to the total mass flow by:

$$W_t = \frac{W_w}{1 - X}$$

where  $X = \frac{H_t - H_w}{H_s - H_w}$ , and

- $X$  = Steam mass fraction ratio;  
 $H_w$  = Specific enthalpy of water (kJ/kg);  
 $H_s$  = Specific enthalpy of steam (kJ/kg).

The specific enthalpies for water and steam should be looked up in steam tables to determine the conditions under which the separator is operated.

## 5.2 Interpretation of output data

Four output characteristic curves were established for well Asal 3 (Figure 13). Two curves at the beginning and at the end of the production test, following the well completion in 1987 by Aquater (Aquater, 1989). Two others curves were obtained by Virkir-Orkint Consulting Group Ltd (1990) during the geothermal scaling and corrosion study. These two periods of production lasted 4 and 3 months, respectively.

Curve 1 (Aquater) represents the results obtained from a water-fed well, feeding from a reservoir of low permeability. After four months, curve 2 was obtained (Aquater) in Figure 12. It indicates about 30-40% decrease in flowrate. The correlation between the second deliverability curve from Aquater 1987 and the first curve 1 from Virkir-Orkint is relatively good. Between these two periods, the well was shut-in. The second curve from Virkir-Orkint shows about 25-28% decrease in the flowrate compared to the earlier curve. Therefore, both phases of production of well Asal 3 show a decrease of 50-60% in its initial output.

Scaling and reservoir pressure drop explain the decrease in flowrate. At the flash zone between 650 and 750 m, the diameter of the wellbore was reduced by about 20 mm. And between 600 m and the wellhead, the diameter reduction was around 15 mm. At low pressure in surface equipment the main deposition was  $\text{FeSiO}_3$  and at high pressure (i.e. down in the well) it was galena  $\text{PbS}$  (Figure 14).

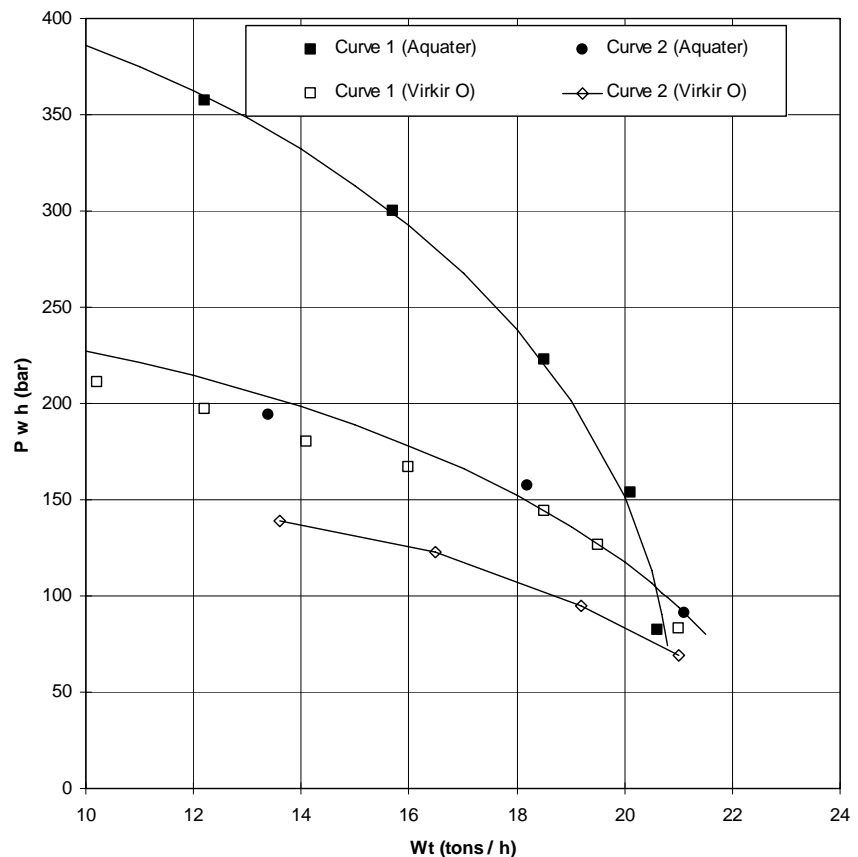


FIGURE 13: Output characteristic curves of well Asal 3 for different tests of well Asal 3

### 5.3 Wellbore simulation

The simulator HOLA was used to simulate the wellbore conditions that influence the transport of fluid from the reservoir to the surface during discharge testing of Asal 3. The simulator numerically solves a set of differential equations that describe the steady-state energy, mass and momentum flow in a vertical pipe for single or two-phase flow. The governing steady-state differential equations for mass, momentum and energy fluxes in a vertical well are (Björnsson et al., 1993):

$$\frac{dW}{dz} = 0$$

$$\frac{dP}{dz} - \left[ \left( \frac{dP}{dz} \right)_{fri} + \left( \frac{dP}{dz} \right)_{acc} + \left( \frac{dP}{dz} \right)_{pot} \right] = 0$$

$$\frac{dE_t}{dz} \pm Q = 0$$

where  $W$  = Total mass flow (kg/s);  
 $P$  = Pressure (Pa);  
 $E_t$  = Total energy flux in the well (J/s);  
 $z$  = Depth coordinate (m);  
 $Q$  = Ambient heat loss over unit distance (W/m).

The plus and minus signs indicate downflow and upflow, respectively. The pressure gradient is composed of three terms: wall friction, acceleration of fluid and change in gravitational load over depth interval (dz).

The governing equation of flow between the well and the reservoir is:

$$W_{feed} = PI \left[ \frac{k_{rw} \rho_w}{\mu_w} + \frac{k_{rs} \rho_s}{\mu_s} \right] * (P_r - P_{well})$$

where  $W_{feed}$  = Feedzone flowrate (kg/s);  
 $PI$  = Productivity index of the feedzone (m<sup>3</sup>);  
 $kr$  = Relative permeability of the phases (subscripts  $w$  for liquid and  $s$  for steam);  
 $\mu$  = Dynamic viscosity (Pa.s);  
 $\rho$  = Density (kg/m<sup>3</sup>);  
 $P$  = Pressure (Pa), subscript  $r$  for reservoir.

Based on the temperature profile during discharge with a 45 kg/s discharge rate (160 tons/h) in Figures 11 and 12, the main feed zone appears to be around 1075 m at 264°C. The data collected during this discharge test are simulated with the HOLA program in order to find the heat losses inside the well (Figure 15).

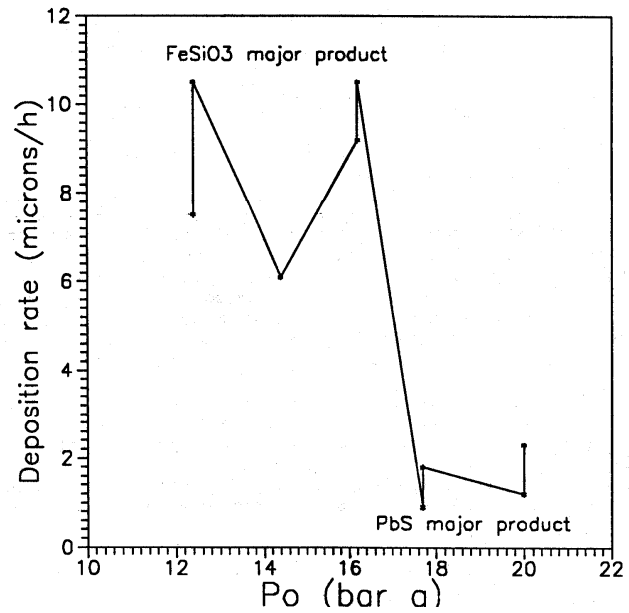


FIGURE 14: Scaling rate at different pressures in well Asal 3

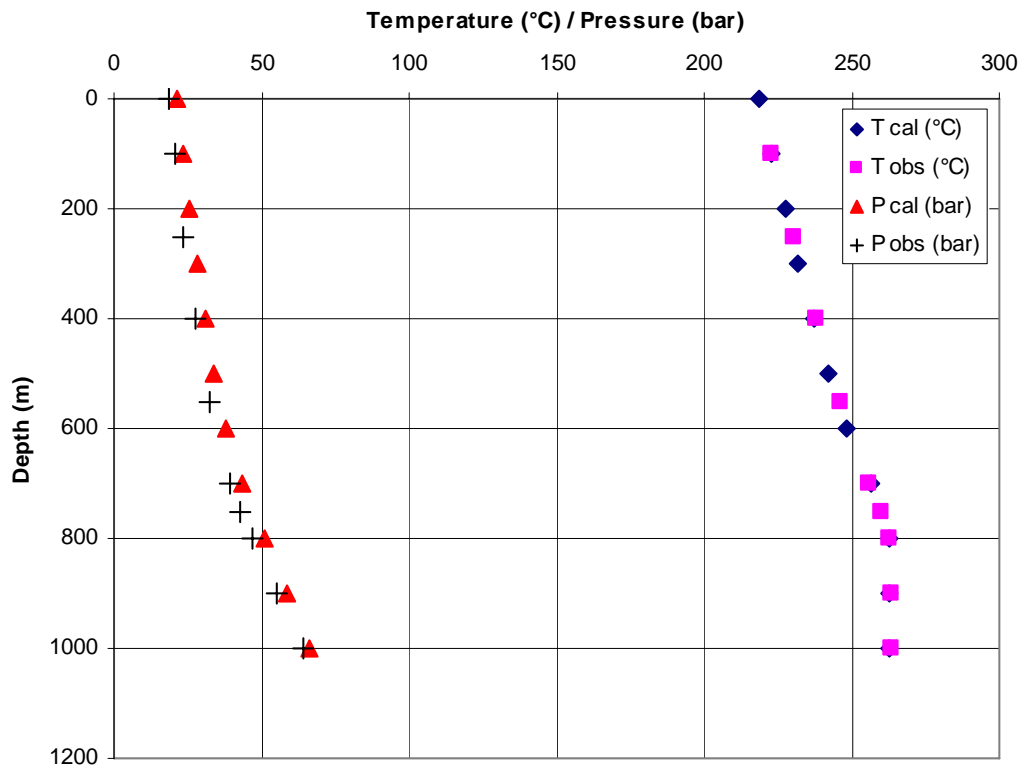


FIGURE 15: Simulation of temperature and pressure profiles for well Asal 3 during 45 kg/s discharge

Simulation was made with no heat exchange between the well and the rock. The difference between the calculated wellhead enthalpy (1140 kJ/kg) and the feed zone enthalpy (1150 kJ/kg) is 10 kJ/kg and the small difference is on the order of the error in the enthalpy estimation. The productivity index estimate is  $2.7 \times 10^{-11} \text{ m}^3$ . This is in a good agreement with the injectivity index obtained by Aquater of  $100 \text{ m}^3/\text{h bar}$ .

## 6. CONCLUSIONS

The main results of the analysis of well test data from the Asal geothermal system presented here are the following:

- The permeability thickness of the deep geothermal reservoir is about 4-8 Dm.
- Based on a porosity of around 10%, and a low storativity value of about  $2 \times 10^{-9} \text{ m}^3$ , a reservoir thickness of about 250 m is estimated.
- During long term exploitation, there is a large drawdown observed in the reservoir.
- The salinity of the deep reservoir fluid in the Asal geothermal field is high (120 g/l).
- Deposition of galena scale inside well Asal 3 while working at high pressure, between 18 and 20 bar-g, reduces the well radius and so decreases the discharge rate.

Based on the reports by Aquater (1989) and Virkir-Orkint (1990), and the results of this work the following recommendations are made:

- Extensive field tests should be performed to obtain more accurate data for estimating the actual size (geophysical exploration) and capacity of the reservoir.

- Since the results of the inhibitor tests made by Virkir-Orkint were relatively promising, laboratory study should be made in order to solve the problem of scaling by finding potential inhibitor chemicals available on the market.
- If the outcome of the above tests is positive, new production wells should be drilled.
- At depths between 400 and 600 m in the Asal area, there is apparently an extensive high-permeability aquifer encountered in all the wells, with a temperature of around 130°C and a salinity content of 50g/l. It is recommended that this aquifer be studied for its suitability for binary power production.

### ACKNOWLEDGEMENTS

I would like to express my gratitude to Dr. Ingvar Fridleifsson and Dr. Jalludin Mohamed for giving me the opportunity to participate in the UNU Geothermal Training Programme in Iceland. I am very grateful to Mr. Lúdvík S. Georgsson and Mrs. Guðrún Bjarnadóttir for kind and patient help during the six months.

I wish to thank my supervisors, Ómar Sigurdsson and Gudni Axelsson, for their continuous supervision and valuable discussions during my work. Finally, I would like to thank all the 2005 UNU Fellows for their friendship and fellow feeling.

### NOMENCLATURE

$A$	= Cross-sectional area of the lip (cm <sup>2</sup> );
$C$	= Wellbore storage coefficient (m <sup>3</sup> /Pa);
$C_D$	= Dimensionless wellbore storage coefficient;
$C_t$	= Total compressibility (Pa <sup>-1</sup> );
$E_t$	= Total energy flux in the well (J/s);
$H$	= Fluid enthalpy (kJ/kg);
$h$	= Thickness (m);
$k$	= Intrinsic permeability (m <sup>2</sup> );
$k_r$	= Relative permeability of the phases;
$m$	= Slope of semi-logarithmic straight line;
$m$	= Slope of multi flowrates;
$P$	= Pressure (Pa);
$PI$	= Productivity index of the feed zone (m <sup>3</sup> );
$P_{lip}$	= Lip pressure at the end of the pipe (MPa);
$P_0$	= Well head pressure (Pa);
$Q$	= Ambient heat loss over unit distance (W/m);
$q$	= Flowrate (m <sup>3</sup> /s);
$r$	= Radial distance (m);
$r_w$	= Wellbore radius (m);
$S$	= Storage coefficient (m/Pa);
$s$	= Skin factor;
$T$	= Temperature (°C);
$T$	= Transmissivity (m <sup>2</sup> /s);
$t$	= Time (s);
$t_D$	= Dimensionless time based on well bore radius;
$V$	= Volume (m <sup>3</sup> );
$W$	= Mass flowrate (kg/s);
$W_{feed}$	= Mass flowrate (kg/s);

$X$	= Steam mass fraction ratio;
$x$	= Horizontal coordinate (m);
$y$	= Horizontal coordinate (m);
$z$	= Vertical coordinate (m);
$\emptyset$	= Porosity
$\mu$	= Dynamic viscosity (Pa s);
$\rho$	= Density (kg/m <sup>3</sup> );

#### Subscripts

$t$	= Total;
$w$	= Water;
$s$	= Steam

## REFERENCES

- Agarwal, R., Al-Hussainy, R., and Ramey H.J., 1970: An investigation of wellbore storage and skin effect in unsteady liquid flow, I. Analytical treatment. *Soc. Pet. Eng. J.*, 5, 279-290.
- Aquater, 1989: *Djibouti geothermal exploration project Republic of Djibouti, final report*. Aquater, report, 159 pp.
- Barberi F., Ferrara G., Santacroce R., and Varet J., 1975: Structural evolution of the Afar triple junction. *Proceedings of the Conference "Afar Depression of Ethiopia", Bad Bergzabben, F.R. Germany, 1974, 1*, 38-54.
- Björnsson, G., Arason, P., and Bödvarsson, G.S., 1993: *The wellbore simulator HOLA. Version 3.1. User's guide*. Orkustofnun, Reykjavík, 36 pp.
- BRGM 1980a: *Asal geothermal field, Republic of Djibouti: analysis of available data* in French. BRGM, report 80SGN525GTH, 42 pp.
- BRGM 1980b: *Report on project DJI78/005. Testing of geothermal fluids, Lac Asal (République de Djibouti): Phase 1* (in French). BRGM, report 80SGN400GTH, 27 pp.
- Correia, H., Fouillac, C., Gerard, A., and Varet, J., 1985: The Asal geothermal field, Republic of Djibouti. *Geothermal Resource Council, Transactions*, 9, 513-519.
- Grant, M.A., Donaldson, I.G., and Bixley, P.F., 1982: *Geothermal reservoir engineering*. Academic Press Ltd., New York, 369 pp.
- Horne, R.N., 1995: *Modern well test analysis, a computer aided approach* (2<sup>nd</sup> edition). Petroway Inc., USA, 257 pp.
- Jalludin, M., 2002: An overview of the geothermal prospections in the Republic of Djibouti. Results and perspectives. *Proceedings of the 2<sup>nd</sup> KenGen Geothermal Conference, Kenya*.
- Theis, C.V., 1935: The relation between the lowering of the piezometric surface and the rate and duration of discharge of a well using ground-water storage. *Transactions, American Geophysical Union*, 16, 519-524.
- Virkir-Orkint 1990: *Djibouti. Geothermal scaling and corrosion study*. Virkir-Orkint, Reykjavík, report, 109 pp.